Bioorganic & Medicinal Chemistry Letters xxx (2013) xxx–xxx

Contents lists available at SciVerse ScienceDirect

Bioorganic & Medicinal Chemistry Letters

journal homepage: www.elsevier.com/locate/bmcl

Design and synthesis of bicyclic heterocycles as potent γ-secretase modulators

Daniel Oehlrich [a,*], Frederik J. R. Rombouts [a], Didier Berthelot [a], François P. Bischoff [a], Michel A. J. De Cleyn [a], Libuse Jaroskova [a], Gregor Macdonald [a], Marc Mercken [a], Michel Surkyn [a], Andrés A. Trabanco [b], Gary Tresadern [a], Sven Van Brandt [a], Adriana I. Velter [a], Tongfei Wu [a], Harrie J. M. Gijsen [a,*]

[a] *Neuroscience, Janssen Research & Development, Turnhoutseweg 30, 2340 Beerse, Belgium*
[b] *Neuroscience, Janssen Research & Development, Jarama 75, 45007 Toledo, Spain*

ARTICLE INFO

Article history:
Received 18 June 2013
Revised 28 June 2013
Accepted 29 June 2013
Available online xxxx

Keywords:
Alzheimer's disease
γ-Secretase modulators

ABSTRACT

The evolution of amide **3** into conformationally restricted bicyclic triazolo-piperidine **14-*S*** as a γ-secretase modulator is described. This is a potential disease modifying anti-Alzheimer's drug which demonstrated high in vitro and in vivo potency against Aβ42 peptide, reduced lipophilicity and enhanced brain free fraction compared to the previous series.

Alzheimer's disease (AD) represents one of the principal unmet medical needs, being the sixth highest cause of death in the US.[1] Presently 30 million people worldwide suffer from AD and this population is predicted to quadruple by 2050. As such this represents a huge social and economic burden.[2] Patients suffering from the disease usually show a gradual decline in their cognitive capabilities, motor and vocal control, which continues with a loss in function of the body and concludes in death. Genetic evidence supports a hypothesis that AD is the result of the formation of Aβ plaques. These are created by the oligomerisation of the Aβ peptides, which then instigate the formation of neurofibrillary tangles and ultimately lead to neuronal death.[3]

The formation of Aβ is a result of the sequential enzymatic cleavage of amyloid precursor protein (APP) initially by aspartyl protease β-secretase 1 (BACE1) and then by γ-secretase, which results in the formation of amyloid peptides of differing lengths. Of these, Aβ42 is the most prone to oligomerisation, and is reported to initiate plaque formation.[4] Post-mortem studies have shown Aβ42 is disproportionately abundant in the amyloid plaques.[4] Due to the biochemical relationship between these enzymes and the onset of AD, BACE1 and γ-secretase have been the target of concentrated research efforts to inhibit the APP processing pathway and thereby prevent pathogenesis and disease progression.[5] This has manifested in increasing reports of optimized BACE1 and γ-secretase inhibitors (GSIs) and more recently, γ-secretase modulators (GSMs).[6–8] GSMs act by reducing the production of the toxic Aβ42 peptides and biasing the APP processing towards shorter length Aβ peptides. Furthermore, GSMs function in such a way that they do not impede the processing of the other γ-secretase substrates, for example Notch, thus resulting in a more optimal phenotype when compared to the traditional GSIs.

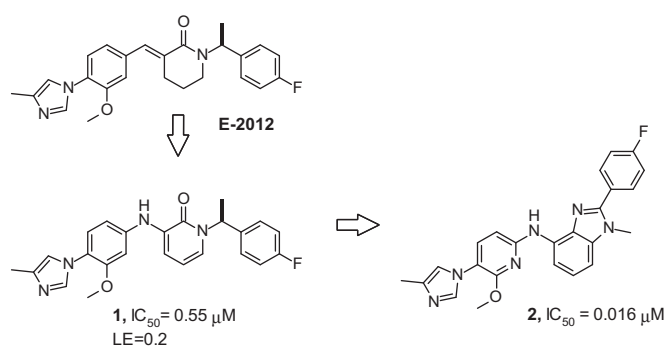

Scheme 1. Ref. 11.

We recently reported the discovery of novel bicyclic heterocycles as potent GSMs derived from conformationally restricted amino-pyridones **1** which in turn were derived from rigidified amides as for example E-2012 (Scheme 1).[9] This investigation culminated in the discovery of benzimidazole **2**, which showed robust in vivo

* Corresponding authors.
E-mail addresses: doehlric@its.jnj.com (D. Oehlrich), hgijsen@its.jnj.com (H.J.M. Gijsen).

0960-894X/$ - see front matter © 2013 Published by Elsevier Ltd.
http://dx.doi.org/10.1016/j.bmcl.2013.06.100

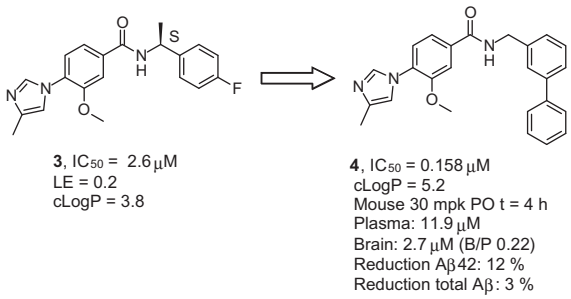

Scheme 2.

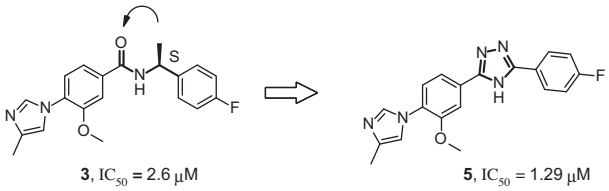

Scheme 3.

lowering of Aβ42 and Aβ40, with the characteristic increase in concentration of the shorter peptides, for example, Aβ37 and Aβ38. Unfortunately, this benzimidazole series suffered from high Log*P* and low solubility, which manifested in signs of liver toxicity.[10]

In parallel we had explored alternative chemical classes, including benzamides represented by **3**.[12] Herein, we disclose the evolution of the amide series into more sophisticated and optimized bicyclic triazoles represented by 1**4**-***S***.[13]

In an effort to identify novel hit series, we performed a *Hit-Hopping* exercise starting with compound **1** with the specific aim to remove unwanted hydrogen bond donors (HBDs) and acceptors (HBAs); this resulted in the identification of simplified amides represented by **3** (Scheme 2). The prototype **3** showed a ~5 fold decrease in activity when compared to **1** (Scheme 1), while maintaining the ligand efficiency (LE = approx 0.2). Further optimization of **3** by the introduction of the 3-phenylbenzylamine substituent led to the potent compound **4** (IC_{50} = 0.158 μM), however this potency increase was achieved at the expense of increasing lipophilicity (**4**, *c*Log*P* = 5.2 vs **3**, *c*Log*P* = 3.8). In mice, after an oral dose of 30 mg/kg, the brain/plasma (B/P) ratio for compound **4** remained limited (B/P 0.22) and no significant reduction of Aβ42 peptide was observed 4 h after administration,[14] despite levels of 2.7 μM being present in the brain.

This result prompted further optimization, with the aim to first increase potency and ultimately brain penetration. In a first exploration, amide **3** was cyclized into a triazole ring **5**. This led to a twofold increase in potency (Scheme 3, Compound **5**, IC_{50} = 1.29 μM).

Assuming the H-bond donor in triazole **5** could limit central penetration, we methylated the triazole nitrogen and obtained a mixture of regioisomers **6** and **7** (Scheme 4). Regio-isomer **6**, was clearly more potent than **7**, and threefold more potent than the non-methylated parent compound **5**. Conformational analysis (Fig. 1 and Supplementary data) suggested the position of the methyl group in **7** was detrimental for activity compared to **6** for two possible reasons. Firstly, the methyl in **7** disturbs the planarity between the triazole and the 4-imidazophenyl ring, the dihedral angle being 45 degrees in **7** compared to 0.5 degrees in **6**. Other literature accounts around similar GSMs suggest torsion and reduction in planarity in this region of the molecule is detrimental for activity.[15,5] It is expected that the acceptor atom (N-4 of the triazole in this case) has to be co-planar with the 4-imidazophenyl ring. Secondly, we have previously discussed the importance of having a twisted or out-of-plane orientation for the distal aromatic group.[9] Indeed, molecule **6** exhibits a twisted orientation of this 4-fluorophenyl ring, whereas for **7** it is planar with respect to the triazole. An analog of **6** having the position of the 4-fluorophenyl and methyl group on the triazole reversed also showed similar potency (Scheme 4, compound **8**).

Given the perceived importance of conformational effects, we targeted molecules with structural motifs which induced low energy conformations with the aforementioned characteristics: namely co-planarity between triazole and 4-imidazophenyl ring whilst a non-planar arrangement between triazole and distal phenyl. Hence, a methylene spacer was introduced between the triazole and the 4-fluorophenyl group (Scheme 5, compound **9**). Unfortunately, this did not result in the anticipated improvement of potency, which was attributed to the conformational freedom of the benzyl group in **9**. To rigidify the structure and optimize the orientation of the 4-fluorophenyl substituent, a 6-membered ring was formed by interconnecting the *N*-methyl group and benzylic position. The resulting compound **10** displayed a significant improvement in potency (IC_{50} = 0.22 μM), consistent with our hypothesis.

Based on our previous experience with GSMs of similar moderate potency, we anticipated that the in vitro activity of **10** would not translate into a significant reduction of Aβ42 in vivo. Hence

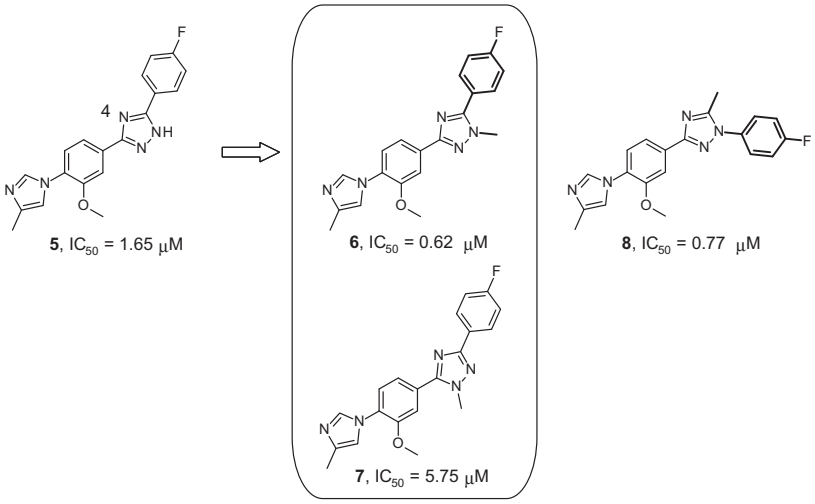

Scheme 4.

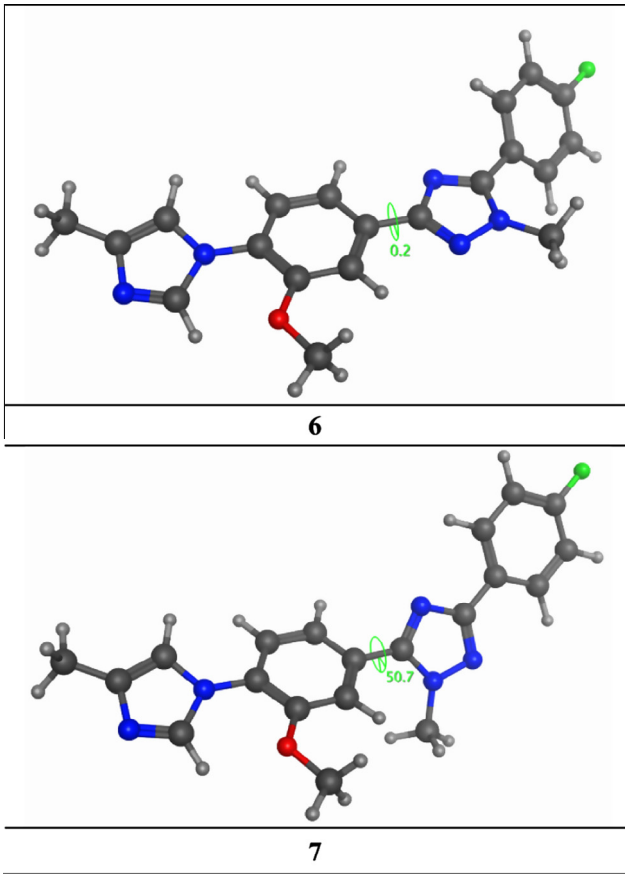

Figure 1. Low energy 3D conformation of molecules **6** and **7**. The lowest energy conformations[16] are shown which maintain an analogous orientation of the triazole. Compound **6** is only 0.001 kcal/mol above the global minimum; compound **7** is 0.2 kcal/mol above global minimum. See Supplementary data for more details.

we continued our research efforts toward more potent analogs. Gratifyingly, a boost in potency was achieved with the introduction of an *ortho*-substituent on the 4-fluorophenyl group giving **11** (IC_{50} = 0.093 μM, racemate). Again, this was possibly due to subtle conformational effects in this region of the molecule. The enantiomers of **11** were separated by chiral SFC to provide **11-*R*** and **11-*S***. Their absolute configuration was determined via VCD (see Supplementary data). Interestingly, **11-*R*** and **11-*S*** display a clear difference in potency of 0.447 and 0.040 μM, respectively (Table 1). Advantageously, the hERG binding opposed the activity of the two enantiomers, with **11-*S*** having an IC_{50} of 7.9 μM while **11-*R*** had an IC_{50} 0.794 μM. The minimum energy conformer of **11-*S*** is shown in Figure 2 and displays many of the features anticipated to be beneficial for GSM activity, such as planarity between the triazole and the 4-imidazophenyl ring, and the out-of-plane twist for

Table 1

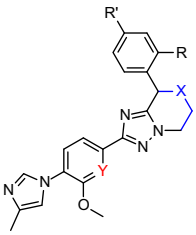

Compound	R	R′	X	Y	Potency IC_{50} (μM)
10	H	F	CH_2	C	0.244
11	Me	F	CH_2	C	0.093
11-*S*	Me	F	CH_2	C	0.040
11-*R*	Me	F	CH_2	C	0.447
12-*S*	CF_3	H	CH_2	C	0.024
13-*S*	CF_3	H	O	C	0.071
14-*S*	CF_3	H	CH_2	N	0.028

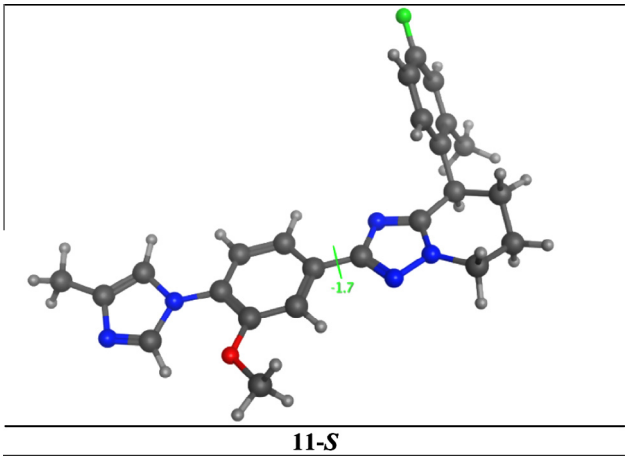

Figure 2. Lowest energy 3D conformation of molecule **11-*S***. See Supplementary data for more details.

the distal phenyl group, in this case promoted by the *ortho* methyl substituent.

Conversion of the *ortho*-methyl to a trifluoromethyl group gave compound **12-*S*** which resulted in a further increase in potency. This also resulted in an unfavorable rise in *c*Log*P* and considerable inhibition of the CYP 3A4 isoform (Table 2, IC_{50} = 0.1 μM). To further improve the physicochemical properties, in particular the lipophilicity and remove potential sites of metabolism, compound **13-*S*** was synthesized, in which the bicyclic piperidine ring was converted to a morpholine. This resulted in a slight drop in potency, but did have the desired effect on *c*Log*P*. (Tables 1 and 2). The decrease in potency suggests an added value created by the

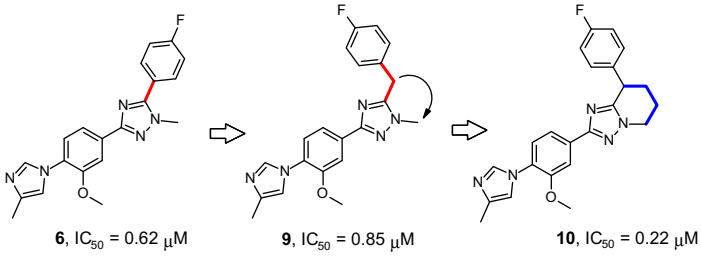

Scheme 5.

Table 2
Profile of compounds **11-*S*** to **14-*S***

	11-*S*	**12-*S***	**13-*S***	**14-*S***
IC_{50} (μM)	0.040	0.024	0.071	0.028
hLM[a]	41	13	5	10
mLM[a]	9	7	6	6
CYP450 IC_{50}. (μM)				
3A4	6.94	0.1	1.10	>10
2C19	9.24	>10	1.52	>10
2C9	5.66	4.64	8.43	8.51
2D6	>10	>10	>10	>10
1A2	>10	>10	>10	>10
hHerg IC_{50}[b] (μM)	7.94	>10	>10	>10
hERG Patch-Xpress inh. at 3 μM[c]	28%	11%	12%	25%
Fu hPlasma[d]	2.7%	ND	ND	8.5%
Fu Brain[e]	0.92%	ND	ND	2.2%
Concd Mouse Plasma 30 mg/kg, 4 h	9.8 μM	9.7 μM	3.6 μM	12.3 μM
Concd Mouse Brain 30 mg/kg, 4 h	4.8 μM	12.7 μM	3.36 μM	2.8 μM
B/P ratio mouse 4 h	0.50	1.29	0.93	0.23
Mouse Aβ42 lowering, 30 mg/kg, 4 h[f]	49%	46%	22%	62%
Mouse Aβ38 increase, 30 mg/kg, 4 h[f]	59%	44%	17%	66%
*c*Log*P*	4.6	4.9	3.4	4.5

[a] % Metabolized after 15 min upon incubation with human (hLM) and mouse (mLM) liver microsomes at 1 μM concentration.
[b] Receptor binding on the human Herg ion channel.
[c] % inhibition of IKr current at 3 μM.
[d] Unbound fraction to human plasma proteins.
[e] Unbound fraction to rat brain tissue.
[f] % Inhibition of Aβ peptides as determined by ELISA.[14]

Table 3
Dog profile of compound **14-*S***

Dog plasma 20 mg/kg @ 8 h	8670 ng/mL, 19 μM
CSF Aβ42 lowering 20 mg/kg @ 8 h	50%
CSF Aβ38 increase 20 mg/kg @ 8 h	28%

hydrogens on the phenethylic carbon, perhaps promoting more of a twisted conformation of the distal phenyl. In an attempt to positively modulate the lipophilicity while maintaining potency, we envisaged that the replacement of the methoxy-phenyl ring by a methoxy-pyridyl would have beneficial effects. Thus, as we previously observed during our optimization towards

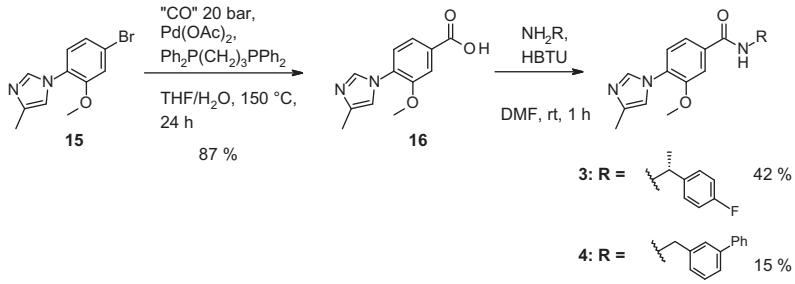

Scheme 6. Synthesis of benzamides **3** and **4**.

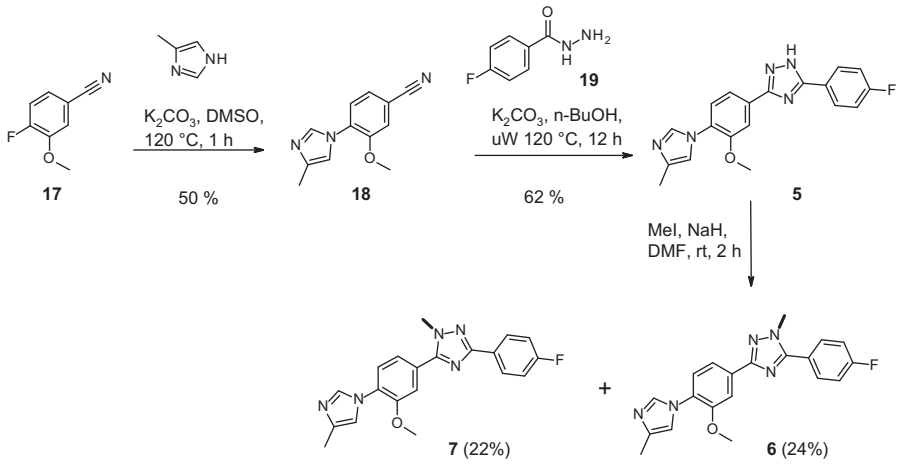

Scheme 7. Synthesis of triazoles **5**–**7**.

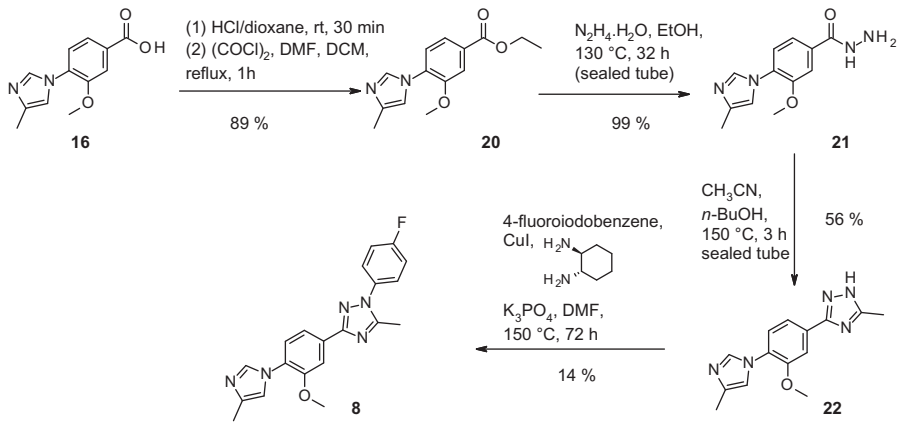

Scheme 8. Synthesis of triazole **8**.

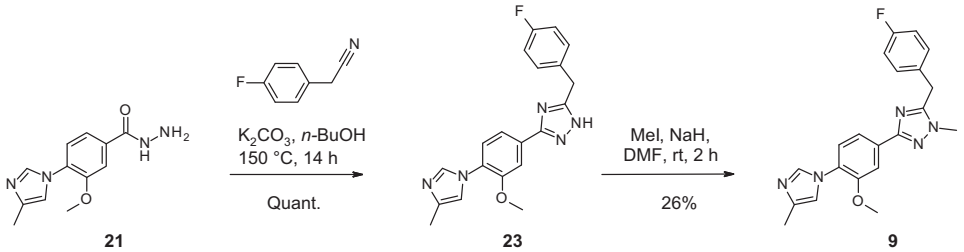

Scheme 9. Synthesis of triazole **9**.

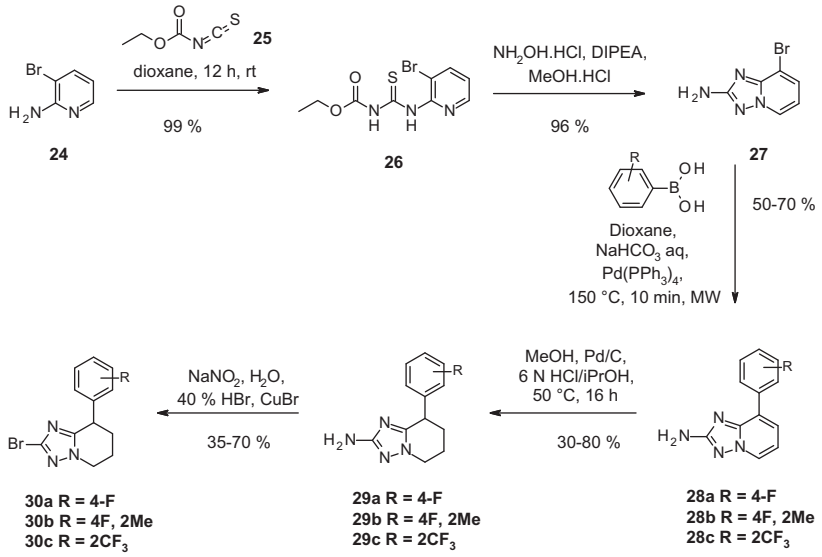

Scheme 10. General synthesis of 5,6,7,8-tetrahydro-[1,2,4]-triazolo[1,5-*a*]pyridine **30a–c**.

benzimidazole **2**,[9] compound **14-*S*** was synthesized, which was found to be equipotent to **12-*S*** while slightly decreasing the *c*Log*P* (Table 2, Compound **12-*S***, *c*Log*P* = 4.9; **14-*S***, *c*Log*P* = 4.5).

When tested orally in mice at 30 mg/kg, **11-*S*** displayed the expected profile of a GSM with a robust reduction of 49% in Aβ42 and 59% increase in Aβ38 and no effect on total concentration of Aβ at 4 h post dosing (Table 2). Bioanalysis showed this effect occurred at a brain concentration of 4.8 μM (B/P = 0.5) and a compound free fraction in brain of 0.92%. The in vitro profile of **11-*S*** showed no major flags apart from mild inhibition of the CYP 2C9 and 3A4 isoforms. These issues were resolved in compound **14-*S***, which also exhibited an increased free fraction in brain of 2.2%. In addition to the improved in vitro profile, compound **14-*S*** demonstrated enhanced in vivo efficacy with a Aβ42 reduction of 62%. This was observed 4 hours post dosing in mice following an oral administration of 30 mg/kg dose. The concentration in the brain at this 4 h time point was 2.8 μM. Unfortunately the B/P ratio had been negatively affected being 0.23.

Compound **14-*S*** was further profiled in the dog (Table 3). An oral dose of 20 mg/kg resulted in a reassuring reduction of 50% in Aβ42 in the cerebrospinal fluid (CSF). The canine model was also used to screen for early effects on liver function.[10] Compound

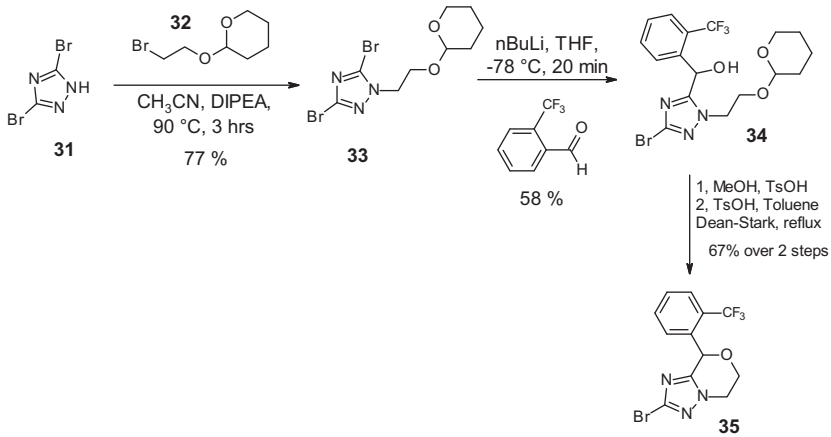

Scheme 11. Synthesis of [1,2,4]triazolo[5,1-*c*][1,4]oxazine **35**.

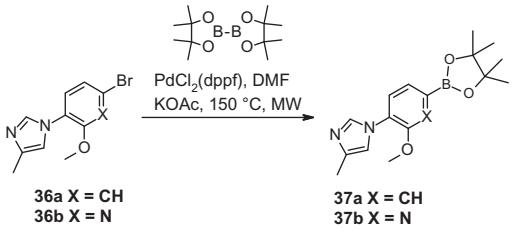

Scheme 12. Formation of pinacol boronate ester **37**.

14-*S* demonstrated clear long-lasting activity, which was seen without increases in the liver function biomarkers bilirubin and alanine transaminase (ALT), despite high compound concentrations/levels. This is considered a clear improvement over GSMs from older series, such as **1** and **2**, which in the same model had shown elevations on bilirubin and/or liver enzymes already at exposure levels below 10 μM.[10]

Chemistry. Compounds **3** and **4** were synthesized from previously reported bromide **15**[9] via Pd catalyzed CO insertion in THF/water to provide acid **16** (Scheme 6). Peptide coupling of **16** with (1*S*)-1-(4-fluorophenyl)ethanamine or 3-phenylbenzylamine gave amides **3** and **4**, respectively, in unoptimised yields.

For the synthesis of triazoles **5**, **6** and **7**, we first substituted 4-fluoro-3-methoxybenzonitrile **17** with 4-methylimidazole to afford intermediate **18** (Scheme 7). Nitrile **18** was condensed with hydrazide **19** to yield triazole **5**. Finally, alkylation of **5** with MeI provided the regioisomeric triazoles **6** and **7** in a 1:1 ratio.

Triazole **8**, was prepared starting from acid **16** (Scheme 8). First, **16** was esterified to **20**. In order to suppress side reactions, **16** had to be used as an imidazolium salt for the esterification, hence **16** was treated with HCl in 1,4-dioxane and evaporated prior to the esterification. Ethyl ester **20** was treated with hydrazine hydrate to provide hydrazide **21**. Condensation of **21** with acetonitrile yielded triazole **22**. Finally a copper-catalyzed arylation of **22** with 4-fluoroiodobenzene provided **8** in 14% yield.

Benzyl analog **9**, was synthesized by reaction of hydrazide intermediate **21** with 2-(4-fluorophenyl)acetonitrile under basic conditions (Scheme 9). The resulting triazole **23** was then alkylated with MeI to afford **9**.

The triazolopyridine core **27** (Scheme 10) was prepared by adding 2-amino-3-bromo-pyridine **24** to isothiocyanate **25** to give **26**, followed by condensation with hydroxylamine to afford bromo derivative **27**. Suzuki–Miyaura cross coupling of **27** to **28** with an appropriately decorated boronic acid, followed by hydrogenation afforded the corresponding bicyclic triazolo-piperidines **29a–c**. Conversion of the amino-triazoles **29a–c** to the corresponding bromo analog **30a–c** was achieved using Sandmeyer conditions.

To form **35**, 3,5-dibromotriazole **31** was alkylated under basic conditions with 2-(2-bromoethoxy)tetrahydropyran **32** giving **33**. Regioselective lithium halogen exchange was achieved by treatment of **33** with *n*-BuLi at −78 °C, which was then quenched by addition of the appropriate aldehyde to afford secondary alcohol **34**. Deprotection followed by condensation using a Dean–Stark apparatus resulted in bicyclic triazolomorpholine **35** (Scheme 11).

Boronate esters **37a** and **37b** were prepared from the previously published bromo-analogs **36a** and **36b** (Scheme 12).[9]

Suzuki–Miyaura cross coupling reactions between boronate esters **37a** and **37b** and bromo-derivatives (**30a–c**, **35**) under

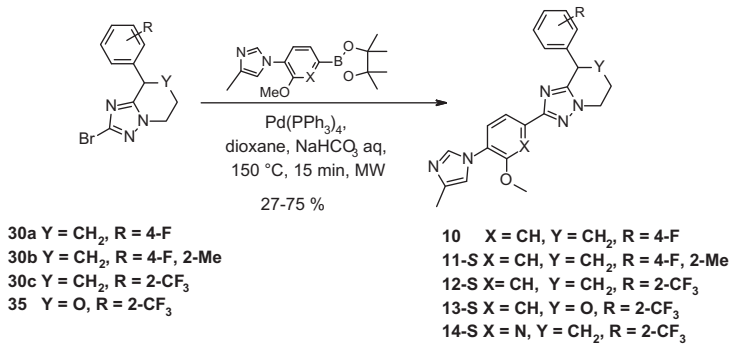

Scheme 13. Synthesis of final compounds **10–14-*S***.

microwave irradiation afforded compounds (**10**–**14**) as racemates. The racemic compounds **11**–**14** were separated by chiral SFC purification to provide the desired enantiomers (**11**-***S***–**14**-***S***) (Scheme 13).

In summary, conversion of amide GSMs into an isosteric triazole, followed by conformational restriction to a bicyclic triazolo-piperidine series resulted in the identification of **14**-***S***. This compound showed potent GSM activity in vitro and in vivo, in combination with an improved drug-like profile compared to previous series. In the dog, at high exposure levels, no effects on liver function were observed, which is most likely due to the reduced lipophilicity of **14**-***S*** compared to previous potent GSMs such as **2** or reported NSAID derived GSMs.[17] These results have strengthened our belief that liver toxicity findings with previous GSMs were not target related and that it should be feasible to develop GSMs without liver toxicity.[18] To achieve significant and sustained changes in Aβ-levels, still high, >10 μM levels of **14**-***S*** were required. There is a growing consensus that amyloid targeting therapies will need to be given early and chronically to have an impact on the progression of AD.[19] Therefore, a further leap in efficacy will likely be required to make GSM treatment a viable option. Considering further optimization of **14**-***S***, an improvement in brain penetration may help to achieve this.

Acknowledgments

The authors would like to thank co-workers at Cellzome, the members of the Janssen R&D Biology, ADME and screening departments and the members of the analysis and purification department.

Supplementary data

Supplementary data (comparison of low energy conformations for molecule **6**, **7** and **11**-*S* and the calculated and determined VCD spectra of **11**-**S** and **11**-*R*) associated with this article can be found, in the online version, at http://dx.doi.org/10.1016/j.bmcl.2013.06.100.

References

1. Alzheimer's Association, 2012 Alzheimer's Disease Facts and Figures, *Alzheimer's & Dementia*, Volume 8, Issue 2.
2. (http://www.alzinfo.org/08/alzheimers/world-alzheimers-day) (http://alzheimers.about.com/od/financialissues/a/Costs_Alzheimer.htm).
3. (a) Lahiri, D. K.; Ghosh, C.; Ge, Y. W. *Ann N.Y. Acad. Sci.* **2003**, *1010*, 643; (b) Walsh, D. M.; Selkoe, D. J. *Neuron* **2004**, *44*, 181; (c) Tolia, A.; De Strooper, B. *Semin. Cell Dev. Biol.* **2009**, *20*, 211; (d) Takami, M.; Nagashima, Y.; Sano, Y.; Ishihara, S.; Morishima-Kawashima, M.; Funtamoto, S.; Yasuo, I. *J. Neurosci.* **2009**, *29*, 13042; (e) Hardy, J.; Selkoe, D. J. *Science* **2002**, *297*, 353.
4. (a) Dickson, D. W. *J. Neuropathol. Exp. Neurol.* **1997**, *56*, 321; (b) McKeith, I. G.; Galasko, D.; Kosaka, K.; Perry, E. K.; Dickson, D. W.; Hansen, L. A.; Salmon, D. P.; Lowe, J.; Mirra, S. S.; Byrne, E. J. L.; Lennox, G.; Quinn, N. P.; Edwardson, J. A.; Ince, P. G.; Bergeron, C.; Burns, A.; Miller, B. L.; Lovestone, S.; Collerton, D.; Jansen, E. N.; Ballard, C.; de Vos, R. A.; Wilcock, G. K.; Jellinger, K. A.; Perry, R. H. *Neurology* **1996**, *47*, 1113; (c) Mandal, P. K.; Pettegrew, J. W.; Masliah, E.; Hamilton, R. L.; Mandal, R. *Neurochem. Res.* **2006**, *31*, 1153.
5. Oehlrich, D.; Berthelot, D. J. C.; Gijsen, H. J. M. *J. Med. Chem.* **2011**, *54*, 669.
6. Probst, G.; Xu, Y. Z. *Expert Opin. Ther. Pat.* **2012**, *5*, 511.
7. Hamada, Y.; Kiso, Y. *Expert Opin. Drug Discov.* **2009**, *4*, 391.
8. Gijsen, H. J. M.; Bishoff, F. P. *Annu. Rep. Med. Chem.* **2012**, *47*, 55.
9. Bischoff, F.; Berthelot, D.; De Cleyn, M.; Macdonald, G.; Minne, G.; Oehlrich, D.; Pieters, S.; Surkyn, M.; Trabanco, A. A.; Tresadern, G.; Van Brandt, S.; Velter, I.; Zaja, M.; Borghys, H.; Masungi, C.; Mercken, M.; Gijsen, H. J. M. *J. Med. Chem.* **2012**, *55*, 9089.
10. Borghys, H.; Tuefferd, M.; Van Broeck, B.; Clessens, E.; Dillen, L.; Cools, W.; Vinken, P.; Straetemans, R.; de Ridder, F.; Gijsen, H.; Mercken, M. *J. Alzheimer's Dis.* **2012**, *28*, 809.
11. IC_{50} represents the concentration of a compound that is required for reducing the Aβ42 level by 50%. The values are a mean of at least three determinations. The confidence intervals for the IC_{50} values are 95%.
12. Work around a similar series of benzamides was published recently: Pettersson, M.; Johnson, D. S.; Subramanyam, C.; Bales, K. R.; am Ende, C. W.; Fish, A. B.; Green, E. M.; Kauffman, G. W.; Lira, R.; Mullins, P. B.; Navartnam, T.; Sakya, S. M.; Stiff, C. M.; Tran, T. P.; Vetelin, B. C.; Xie, L.; Zhang, L.; Pustilnik, L. R.; Wood, K. M.; O'Donnell, C. J. *Bioorg. Med. Chem. Lett.* **2012**, *22*, 2906.
13. Wu, T.; Gijsen, H. J. M.; Rombouts, F. J. R.; Bischoff, F. P.; Berthelot, D. J.-C.; Oehlrich, D.; De Cleyn, M. A. J.; Pieters, S. M. A.; Minne, G. B.; Velter, A. I. PCT-WO2011006903.
14. Mouse in vivo at 30 mg/kg oral administration after 4 h ($n = 6$) expressed as a percentage of Aβ42 lowering in brain compared with untreated animals. Plasma and brain samples were analyzed for the tested compound using a qualified research LC–MS/MS method. For a more detailed description of the in vivo and in vitro assays, see Ref. 9
15. Huang, X.; Aslanian, R.; Zhou, W.; Zhu, X.; Qin, J.; Greenlee, W.; Zhu, Z.; Zhang, L.; Hyde, L.; Chu, L.; Cohen-Williams, M.; Palani, A. *ACS J. Med. Chem. Lett.* **2010**, *1*, 184.
16. Conformational analysis was performed in Molecular Operating Environment version 2011.10. Default MMFF94x force field settings were used with Born solvation turned on (internal dielectric 1, external 80). Low mode MD approach was used for the conformational searches, all settings were at default except rejection limit was increased to 1000, inter-conformer RMSD acceptance was set at 0.1 Å and energy window was increased to 10 kcal/mol.
17. Van Broeck, B.; Chen, J.-M.; Tréton, G.; Desmidt, M.; Hopf, C.; Ramsden, N.; Karran, E.; Mercken, M.; Rowley, A. *Br. J. Pharmacol.* **2011**, *163*, 375.
18. Gijsen, H. J. M.; Mercken, M. *Int. J. Alzheimer's Dis.* **2012**, *2012*, 295207.
19. Miller, G. *Science* **2012**, *337*, 790.